e-ISSN: 2564-7954 CUJSE 22(1): 050-062 (2025) Research Article

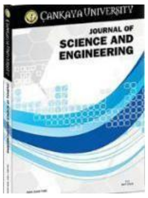

Çankaya University

Journal of Science and Engineering

CUJSE

https://dergipark.org.tr/cankujse

Influence of Surface Condition and Preheating Treatments on the Deposition Characteristics of Cold-Sprayed IN718 Alloy

Seren Özer[1,2], Merve Özkan[3], Arcan F. Dericioğlu[1,*]

[1] Department of Metallurgical and Materials Engineering, Middle East Technical University, Ankara / Türkiye
[2] Department of Metallurgical and Materials Engineering, Atılım University, Ankara / Türkiye
[3] Department of Materials Science and Engineering, Eskişehir Technical University, Eskişehir / Türkiye

Keywords

Cold Spray,
IN718,
Preheating,
Microstructure,
Surface Condition.

Abstract

This study examines the influence of surface condition and preheating treatment on the deposition thickness and uniformity of cold-sprayed Inconel 718 alloy. Three distinct surface finishes were applied to the Inconel 718 substrates: grinding with 60 and 600 SiC grit emery paper, and polishing. Subsequently, some of the substrates were subjected to preheating at 1040 °C for 2 hours to promote improved interfacial bonding between the substrate and the initial layer of deposited particles. The results revealed that the pre-heated Inconel 718 substrate ground with 600 SiC emery paper exhibited a uniform deposition, attaining a maximum thickness of approximately 70 µm. Conversely, interface delamination and crack formation were found in all surface conditions of the non-preheated substrates. However, powder particle detachment was observed in both preheated and non-preheated substrates, which was consistent with the surface morphologies. To enhance interparticle bonding and promote increased deposition thickness, the Inconel 718 powder was preheated at 200 °C for 24 hours. This treatment resulted in a deposition thickness of approximately 160 µm, which can be ascribed to the improved deformability of the powder particles induced by thermal softening mechanism.

1. Introduction

Cold spray process is employed to deposit solid materials in a non-molten state, enabling the surface restoration of components subjected to mechanical- or corrosion-induced damage, the development of protective coatings, and the manufacturing of freestanding structures [1]. In this system, a high-temperature compressed gas (e.g., air, nitrogen, helium, or their mixture) is utilized to accelerate feedstock powder particles, typically ranging from 1 to 50 µm in diameter, through a converging-diverging nozzle. As the gas expands, its velocity increases substantially, propelling the particles toward the substrate at supersonic velocities. Upon impact, the high kinetic energy of the particles induces severe plastic deformation, promoting both metallurgical and mechanical bonding, which facilitates the formation of a dense and well-adhered coating [2] [3]. This method provides significant advantages over conventional thermal spray deposition. The relatively low processing temperatures preserve the intrinsic properties of the feedstock powders while minimizing oxidation and microstructural changes, such as phase transformations, thereby improving coating durability [4]. Furthermore, the compressive residual stresses

*Corresponding Author: arcan@metu.edu.tr
Received: April 8, 2025, Accepted: April 29, 2025

induced on the substrate surface, as opposed to the tensile stresses typically observed in additive manufacturing techniques, enhance the mechanical properties and wear resistance of the cold-sprayed deposits [5]. Another notable feature of this method is its high deposition rate and adaptability to complex geometries, especially when integrated with a robot-controlled spraying system [6]. Due to its beneficial attributes, this technology is extensively used for the fabrication and coating of diverse metallic materials, including soft metals (e.g., Al, Mg, and Cu alloys), hard metals (e.g., Ti-, Fe-, and Ni-based alloys), metal matrix composites, and amorphous alloys [7].

Inconel 718 (IN718), a precipitation-hardenable Ni-based superalloy, is extensively employed in aerospace and gas turbine applications due to its outstanding creep and fatigue resistance, high-temperature mechanical properties, and superior corrosion and oxidation resistance in extreme environments [8]. The primary strengthening mechanism of IN718 arises from the formation of body-centered tetragonal (BCT) γ'' (Ni_3Nb) precipitates, while the $L1_2$-ordered γ' ($Ni_3(Al,Ti)$) phase and carbides provide a secondary strengthening contribution to the γ matrix [9]. This alloy retains its structural integrity at service temperatures up to approximately 650 °C; however, prolonged exposure may lead to phase instability, microstructural degradation, and loss of mechanical properties [10]. Under these circumstances, repairing damaged IN718 components is often a more cost-effective alternative to complete replacement.

In the cold spray process, the formation of the deposit involves two distinct stages: (i) initial layer deposition, where bonding is achieved through the interaction between the substrate and impacting particles, and (ii) subsequent layer build-up, where bonding occurs between feedstock particles [11]. It should be emphasized that these mechanisms are primarily influenced by the surface condition and processing factors, including propulsive gas and nozzle parameters, along with characteristics of the feedstock powders and substrate materials [12]. The surface condition of the substrate is one of the key factors governing particle adhesion and overall deposition efficiency, as it directly affects residual stress distribution and defect formation [13]. It is widely recognized that surface roughening before deposition enhances coating adhesion by increasing the interaction area and promoting an oxide-free surface [14]. Another approach for strengthening the bonding mechanism and enhancing the quality of cold-sprayed deposits involves preheating the substrate or feedstock powder, which reduces resistance to plastic deformation through thermal softening [15]. Singh et al. [14] examined the effects of surface roughness on the deposition behavior of IN718 powder by analyzing single-particle interactions with an IN718 substrate. Their findings revealed that a reduction in surface roughness constrained localized plastic deformation and interfacial material mixing, thereby facilitating the formation of defects such as cracks, pores, and delamination. Conversely, Sun et al. [16] demonstrated that polishing the IN718 substrate to achieve a smooth surface facilitated adiabatic shear instability and material jetting, thereby enhancing bonding strength. Furthermore, they investigated the effect of preheating the IN718 substrate at 25, 100, 200, and 450 °C on the deposition mechanism. They observed that without preheating, the interface contained gaps and cracks, signifying insufficient bonding between the substrate and deposited particles. In contrast, higher preheating temperatures facilitated the formation of jetting phenomena, indicative of enhanced metallurgical bonding, as validated by shear test results. In another study, Xie et al. [17] investigated the impact of particle preheating on the deposition mechanism by heating Ni particles to 473, 673, and 873 K before their deposition onto Al substrate. They observed that appropriate preheating enhanced the adhesion strength of the deposition, with 473 K determined as the optimal temperature. As previously noted, the formation of an oxide-free interface is crucial for ensuring effective metal-to-metal contact between particles and the substrate, which directly influences deposition efficiency. However, microstructural analysis revealed oxide film debris at the Ni-Al interface, significantly weakening metallurgical bonding. This deterioration led to the formation of discontinuous diffusion coating and defects, particularly at elevated preheating temperatures.

The findings emphasize the significance of investigating the effects of surface condition and preheating treatments on the deposition behavior of cold-sprayed IN718 substrates. While surface condition plays a critical role in substrate-particle interactions, a preheating process is essential for enhancing interfacial and interparticle bonding mechanisms, thereby improving deposition quality and structural coherence. In this context, IN718 powder and IN718 substrates with various surface conditions were subjected to preheating treatments to improve deposition efficiency.

2. Experimental Procedure

2.1. Feedstock Powder

Commercial gas-atomized IN718 particles, obtained from Oerlikon Metco Co. and ranging in size from 15 to 45 μm, were utilized as feedstock powder for cold spray processing. The chemical composition of the powder (Table 1) was verified through energy dispersive spectroscopy (EDS) analysis using a scanning electron microscope (SEM) (ZEISS Merlin® FE-SEM, Germany) and was found to comply with the AMS 5383 standard [18]. As shown in Figure 1(a, b), the powder predominantly exhibits a spherical morphology, with some satellite particles likely formed due to the rapid solidification inherent in the gas atomization process [19].

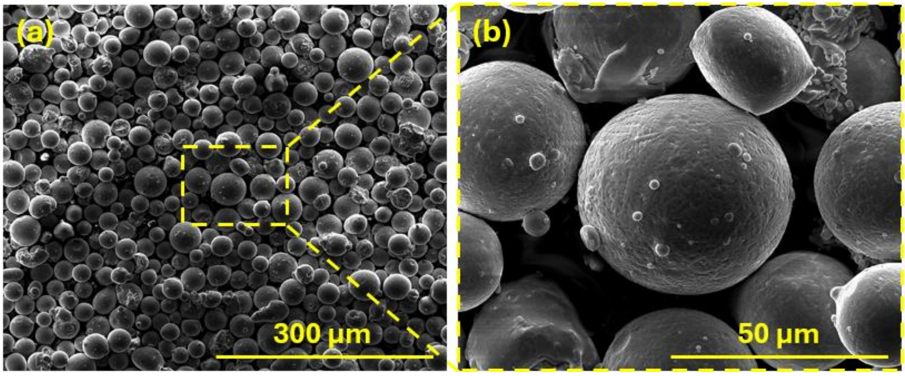

Figure 1. (a, b) SEM images of IN718 powder employed in the cold spray process.

Table 1. Compositional analysis of IN718 powder in comparison with AMS 5383 standard.

	Elements (wt. %)						
Material	**Ni**	**Cr**	**Nb**	**Mo**	**Ti**	**Al**	**Fe**
Powders used in the cold spray deposition	52.64	19.42	5.17	3.18	1.03	0.61	Bal.
AMS 5383 Standard	50-55	17-21	4.75-5.5	2.8-3.3	0.65-1.15	0.2-0.8	Bal.

2.2. Production and Preparation of IN718 Substrates

Cylindrical IN718 substrates, with dimensions of 120 mm in height and 15 mm in diameter, were fabricated using an Arcam A2X Electron Beam Melting (PBF-EB) system under a constant gun-accelerating voltage of 60 kV. The process was conducted in a controlled vacuum environment, utilizing high-purity helium as a regulating gas to prevent oxidation-and contamination-related issues. Furthermore, a preheating temperature of 1025 °C was applied during the initial stages of processing to minimize thermal gradients between the build platform and the fabricated components. The specific process parameters employed in manual mode for substrate fabrication are summarized in Table 2. The selection of processing parameters was guided by an in-depth review of existing literature, with a focus on conditions that effectively suppress the formation of detrimental defects such as cracks. For instance, Lee et al. [18] demonstrated that IN718 produced via PBF-EB with higher beam currents (18 mA) achieved significantly higher relative densities, up to 99.96%, compared to samples produced using lower beam currents (12 mA). The line-offset and layer thickness parameters are commonly applied in accordance with the guidelines provided by Arcam for the production of IN718 alloy, as also observed in the study conducted by Deng et al. [19]. Furthermore, Im et al. [20] reported that a scanning speed within the range of 500 to 6000 mm/s is applicable and identified a scanning speed of 4500 mm/s as the optimal condition to achieve a relative density exceeding 99.9%.

Table 2. PBF-EB process parameters utilized in the fabrication of IN718 substrates

Beam current (mA)	Scan speed (mm/s)	Line-offset (mm)	Layer thickness (mm)
18	4530	0.125	0.075

For cold spray processing and microstructural analysis, the samples were sectioned into 10 mm thick slices using a precision abrasive cutter (Buehler IsoMet 5000). Prior to deposition, the substrate surfaces were ground using P60 and P600 grade SiC sandpapers, while some samples were further polished with 9, 3 and 1 µm diamond suspensions to assess the effect of surface condition. Subsequently, all samples were ultrasonically cleaned in acetone for 15 minutes.

2.3. Cold Spray Deposition

The cold-sprayed IN718 deposits were fabricated using the Dycomet D523 Cold Spray System, which features a Laval-type converging-diverging nozzle with a 6 mm outlet diameter to enhance particle acceleration. Additionally, compressed air was used to prevent nozzle clogging, while nitrogen gas served as the propellant, with an inlet temperature of 600 °C and a pressure of 2 MPa. The deposition of the substrates was performed using the following process parameters: a stand-off distance of 20 mm, a nozzle traverse speed of 5 mm/s, a scanning step of 2 mm, a spray angle of 90°, and a total of five cycles.

2.4. Heat Treatment Procedure

To enhance the deformability of the alloy, both the substrate and powder were subjected to preheating treatments. The IN718 substrates underwent solution treatment at 1040 °C for 2 hours, followed by air cooling to reduce hardness and homogenize the microstructure before cold spray processing. Meanwhile, the IN718 powder particles were preheated at 200 °C for 24 hours under vacuum conditions, with the aim of relieving internal stress and enhancing particle deformability upon impact. From this point onward, the as-fabricated and pre-heated samples were designated as ASF and PH, respectively. The abbreviations of the samples and their corresponding surface conditions are detailed in Table 3.

Table 3. The sample abbreviations and their corresponding surface conditions

Sample	Description
ASF	As-fabricated IN718 substrate (no prior treatment, as-fabricated condition)
ASF-60	ASF-IN718, ground with 60 grit emery paper
ASF-600	ASF-IN718, ground with 600 grit emery paper
ASF-P	ASF-IN718, polished surface
PH	Pre-heated IN718 substrate
PH-60	PH-IN718, ground with 60 grit emery paper
PH-600	PH-IN718, ground with 600 grit emery paper
PH-P	PH-IN718, polished surface

2.5. Characterization Methods

Microstructural observations of the cold-sprayed and pre-heated powder were conducted using a scanning electron microscope (SEM) (Nova NanoSEM 430, FEI Company) operated at an accelerating voltage of 20 kV, along with a high-capacity digital microscope (HDS-5800, Huvitz Corp.). Prior to analysis, the cross-sections of the substrates were prepared using standard metallographic procedures, including mounting, grinding, and polishing. Following cleaning with deionized water and ethanol, the deposited substrates were etched with Kalling's reagent (40 mL HCl, 2 g $CuCl_2$, and 40 mL ethanol) for 30–50 seconds.

The average surface roughness (Ra) of the substrates under varying conditions was measured using a surface profilometer (Mitutoyo SJ-400) equipped with a 2 μm diameter diamond stylus. Roughness measurements were conducted in two distinct regions of each substrate, covering an area of 10×10 mm².

X-ray diffraction (XRD) analyses were performed using a Rigaku DMAX 2200 diffractometer to identify secondary phases or oxides present in the substrates. The measurements were carried out with Cu-Kα radiation ($\lambda = 1.5406$ Å) under operating conditions of 40 kV and 30 mA, employing a constant scan rate of 0.5 °/min.

3. Results and Discussion

3.1. Effect of Surface Conditions and Substrate Preheating on Deposition Thickness

The initial series of deposition processes was conducted to investigate the influence of the substrate preheating and surface conditions on coating thickness and quality. For this purpose, the ASF and PH substrates were prepared with three distinct surface conditions: ground with P60 SiC sandpaper, ground with P600 SiC sandpaper, and polished. Figure 2 presents optical images of cold-spray deposited ASF and PH substrates with varying surface conditions. The average surface roughness (Ra) values of the IN718 substrates, designated as ASF-60 and ASF-600, were measured as 0.50 ± 0.08 μm and 0.09 ± 0.01 μm, respectively, whereas the polished substrate (ASF-P) exhibited a considerably lower roughness of 0.016 ± 0.014 μm. As shown in Figure 2(a), the ASF-60 substrate exhibited the lowest deposited thickness, approximately 10 μm, with a non-uniform distribution. On the other hand, the ASF-600 and ASF-P substrates demonstrated higher deposit thicknesses, measuring approximately 40 μm and 20 μm, respectively. However, as illustrated in Figures 2(b, c) and 3(a), delamination of the deposited layer was clearly observed, indicating poor adhesion to the substrate. This detachment may be attributed to inadequate impact-induced deformation or poor interfacial bonding between the powder particles and the substrates.

While certain studies have reported that grit-blasting enhances deposition efficiency, others have found that surface preparation methods such as grinding or polishing improve coating-substrate bonding strength compared to grit-blasted substrates. For example, Kumar et al. [21] found that the bonding strength of Cu-on-Al and Cu-on-Cu interfaces was reduced under polished conditions compared to grit-blasted surfaces. Additionally, the finite element analysis results indicated that frictional dissipation, arising from the conversion of kinetic energy into heat due to friction between the impacting particles and the rough substrate, leads to increased interface temperatures, which, in turn, enhance interfacial bonding. However, it is important to note that grit-blasting or rough grinding may increase the hardness of the substrate due to work hardening, which can limit its deformability. Another consideration for grit-blasted surfaces is that the rough texture can act as a stress concentration site, promoting crack initiation and propagation, which ultimately leads to a decrease in the overall performance of the deposited parts [22]. Conversely, Bisht et al. [23] revealed that increasing surface roughness, as observed in grit-blasted substrates, restricts particle deformation due to reduced particle velocity, resulting in poor interfacial bonding compared to the ground and polished counterparts. On the other hand, Tan et al. [24] reported that a fine-ground Ti6Al4V substrate coated with same material demonstrated improved deposition efficiency, as well as the absence of cracks and interface delamination. Moracco et al. [25] also found that the ground and polished Ti6Al4V substrate achieved a bond strength of approximately 22 MPa, which was significantly higher than the bond strength of about 8 MPa observed for grit-blasted substrates. As demonstrated in this study, a relatively rough surface, approximately 0.1 μm in Ra, could be essential for achieving effective deposition in hard-to-hard materials such as IN718.

Further SEM investigations were carried out to perform a comprehensive defect analysis of the ASF-600 sample. As presented in Figure 4, two separate deposition zones are identified, each exhibiting different types of defects induced by the cold spray process. Figure 4(a) reveals that the deposited layer partially detached from the substrate surface, leading to the formation of an interfacial crack. Moreover, Figure 4(b) displays several interfacial voids, with lengths reaching up to 10 μm, observed on the other side of the deposition. Upon examination of the deposition characteristics, it was observed that the IN718 powder particles underwent significant plastic deformation during the cold spray process, resulting in the formation of elongated grains exhibiting a fine cellular and dendritic microstructure within the deposited material. Furthermore, numerous white particles observed along the boundaries were identified as Laves phases enriched in Nb and Mo, along with the presence of some carbides, as confirmed by the EDS mapping analysis. These secondary phase particles were also present along the interface boundary, which may contribute to the poor bonding between the deposition and the substrate. Additionally, some inter-splat voids were found between the deformed particles, suggesting potential areas of weak inter-particle adhesion that negatively impact the deposition quality.

As previously discussed, the bonding mechanism in cold spray processing involves two distinct stages: the initial bonding between the first layer of deposited particles and the substrate, which facilitates adhesion, and the subsequent bonding between progressively deposited layers, which is responsible for cohesion [26]. The initial bonding, induced by high-velocity impacts, primarily results from metallurgical and mechanical interlocking, further enhanced by mechanisms such as adiabatic shear instability (ASI) and material jetting [27]. Severe plastic deformation of the material in the solid state, accompanied by high strain, generates localized heating, which subsequently induces ASI on the substrate surface, resulting in material flow at the interface. This phenomenon can be described by three primary mechanisms: (i) a substantial increase in the interfacial contact area, (ii) localized material mixing facilitated by shear band formation due to recrystallization, or even localized melting, and (iii) the formation of metallurgical bonds promoted by intense plastic deformation [28]. Fardan et al. [29] reported that material jetting occurs when ASI exceeds the strain hardening rate, resulting in mechanical interlocking. Upon impact, the substrate material undergoes localized deformation, resulting in the formation of protrusions that partially envelop the particles, thereby improving interfacial bonding between the initial layer of deposited powder and the substrate [30]. However, the findings revealed no evidence of jetting formation on the surface of the ASF substrates, as illustrated in Figures 2–4, suggesting inadequate bonding in the as-fabricated condition. It is well recognized that substrate preheating plays a crucial role in promoting the occurrence of ASI mechanisms [16]. The results revealed that the PH substrates showed improved adhesion and more uniform deposition, suggesting that preheating enhances bonding between the deposited powder and the substrate. As shown in Figure 2(d, f), the deposit thickness for the PH-60 and PH-P substrates was similar, ranging between 20 and 30 μm. Notably, the PH-600 substrate achieved the maximum deposit thickness, approximately 70 μm, as depicted in Figure 2(e, e1, and e2). However, the PH-600 substrate also demonstrated detachment along the interface, although the extent of delamination appears to be reduced compared to ASF-600, as shown in Figure 3(b). In a study conducted by Yu et el. [15] indicated that an increase in preheating temperature enhances the impact velocity, resulting in the formation of deeper craters on the surface due to the improved deformability of the substrate. A similar study was performed by Garfias et al. [31]; however, their preheating temperatures of 250 and 400 °C were considerably lower than those used in the present study. They reported that preheating the substrate to 400 ºC promoted the formation of a dense deposition with a thickness of 1.2 mm, resulting in an adhesion strength exceeding 50 MPa.

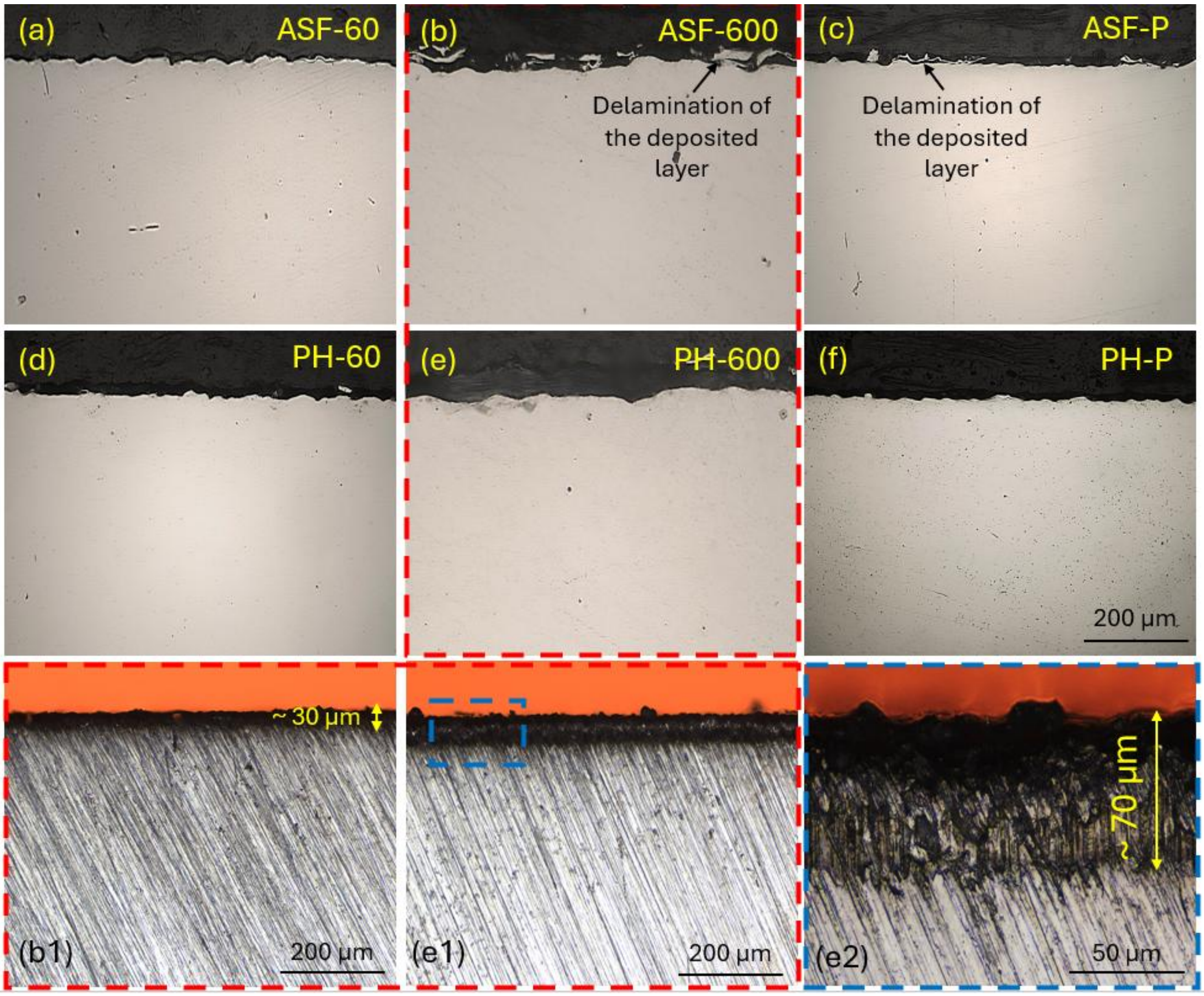

Figure 2. Optic images of the cold-spray deposited substrates: (a) ASF-60, (b) ASF-600, (c) ASF-P, (d) PH-60, (e) PH-600 and (f) PH-P. (P: polished condition)

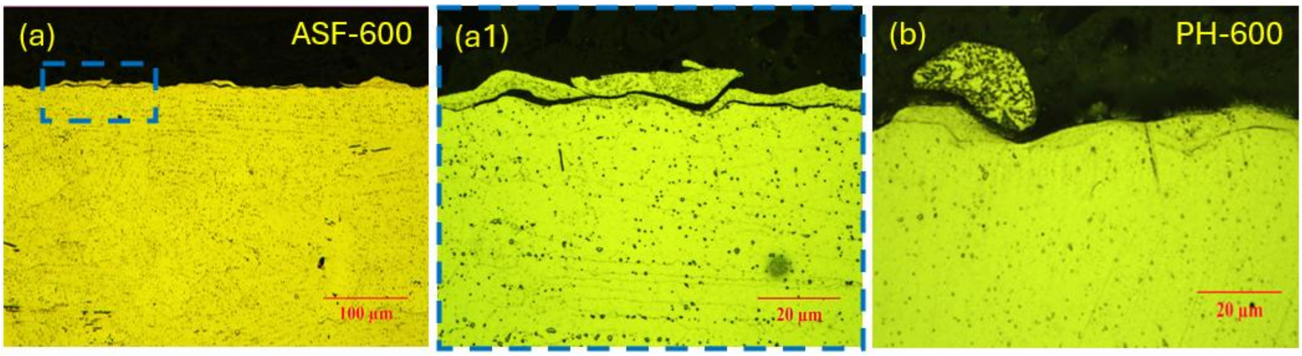

Figure 3. Optical images illustrating the delamination of the deposited layer from the substrate surface: (a) ASF-600 and (b) PH-600.

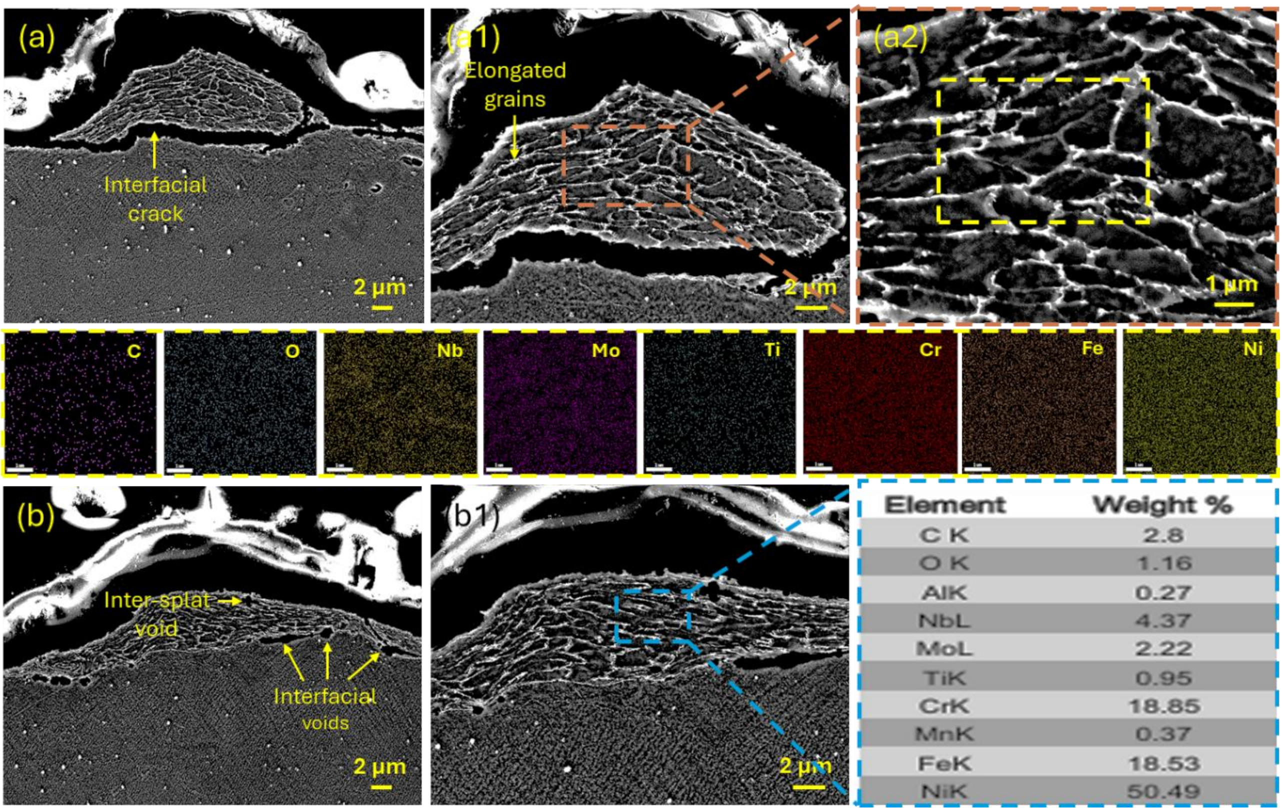

Element	Weight %
C K	2.8
O K	1.16
AlK	0.27
NbL	4.37
MoL	2.22
TiK	0.95
CrK	18.85
MnK	0.37
FeK	18.53
NiK	50.49

Figure 4. (a) and (b) SEM images and corresponding EDS mapping analysis of the ASF-600 substrate, illustrating the splat boundaries within the deposition and interfacial defects.

3.2. Effect of Particle Preheating on the Deposition Thickness

It is important to emphasize that the deformability of powder particles is as crucial as that of the substrate in achieving effective bonding and deposition integrity during cold spray processing. As seen in Figure 5, the surface morphology of the ASF-600 and PH-600 substrates revealed that while the deposited layers exhibited uniformity, some powder particles had detached from the substrate surfaces, leading to the formation of craters on both substrates. To enhance particle-particle interactions and promote thicker deposition, the as-received IN718 powder particles underwent a preheating treatment at 200 °C for 24 hours. This treatment aimed to reduce internal stress, improve particle deformability upon impact, and facilitate stronger interparticle bonding during the deposition processing.

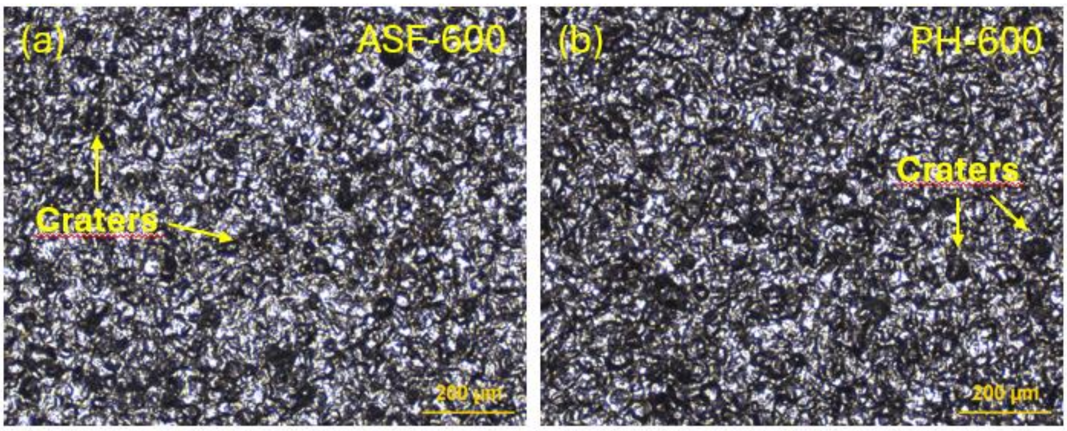

Figure 5. Optic images showing surface morphologies of the deposited substrates: (a) ASF-600 and (b) PH-600.

One of the main reasons for selecting this temperature, which is considerably lower than the alloy's solvus temperature, is to effectively minimize the risk of substantial microstructural changes. According to the time-temperature-transformation (TTT) behavior of the IN718 alloy, the precipitation of γ′, γ″, and δ (Ni_3Nb) phases, along with Nb-rich carbides, occurs at temperatures up to 1000 °C. Depending on their characteristics, these phases can lead to a reduction in the deformability of the powder particles, as an increased volume fraction contributes to their strengthening. Moreover, embrittlement may occur, which is attributed to the morphology and distribution of the phases. For instance, the formation of needle-like δ phases along the grain boundaries facilitates crack initiation and propagation by providing preferential pathways, thereby compromising the alloy's mechanical integrity [32]. Another critical factor is the oxidation of powder particles at temperatures exceeding 1000 °C, which detrimentally influences the bonding mechanism during cold spray processing. This phenomenon promotes the formation of a high density of voids between the plastically deformed particles. In light of the aforementioned challenges, including microstructural instability and the risk of oxidation at elevated temperatures, a relatively low preheating temperature was deliberately selected to mitigate these adverse effects. A prolonged preheating duration of 24 hours was implemented to facilitate the relief of internal stresses generated during the rapid solidification inherent to the gas atomization process. The thermal softening of the powder particles enhanced their plastic deformability, thereby improving interfacial bonding between the substrate and the deposited material. Moreover, this extended thermal treatment contributed to microstructural homogenization and mitigated elemental segregation within the powder particles. As illustrated in Figure 6(a) and further detailed in Figure 1, the as-received IN718 powder predominantly displayed a spherical morphology, with the presence of micron-sized pores within the particles. Following the preheating treatment, the overall particle morphology remained largely unaltered, with no noticeable agglomeration being observed, as depicted in Figure 6(b, c).

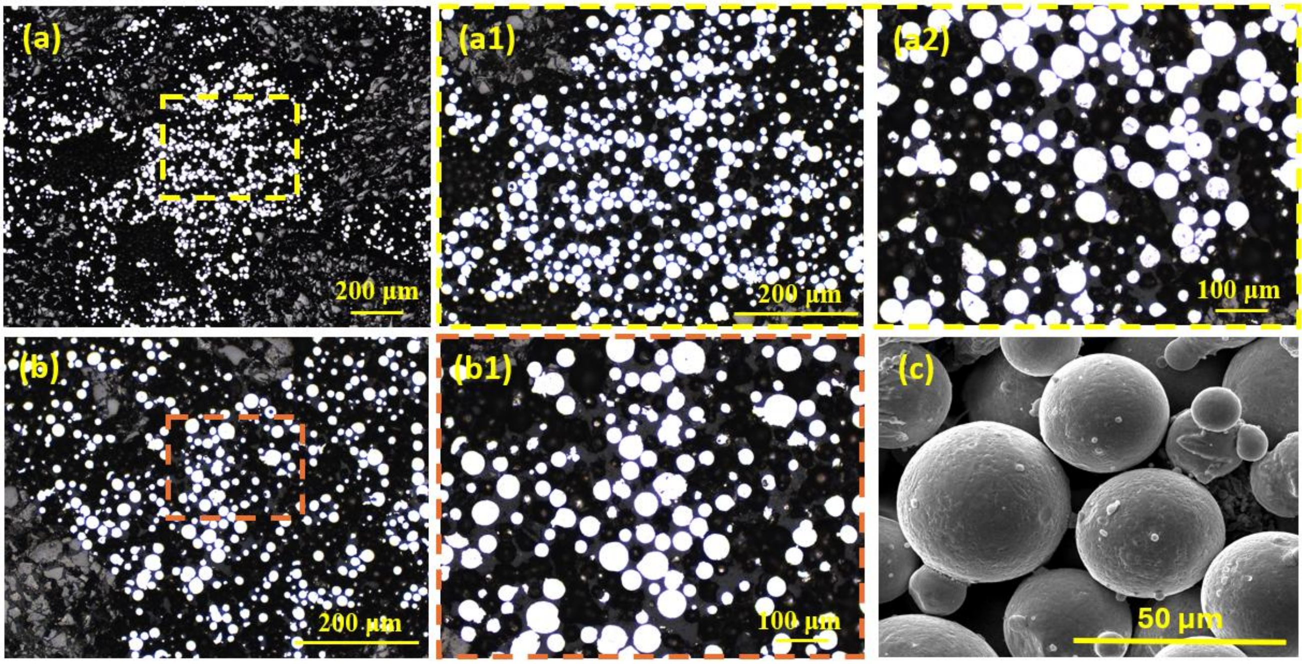

Figure 6. Optic images of the IN718 powders: (a) as-received, (b) pre-heated and (c) SEM image of the pre-heated powder.

To investigate the effect of preheating on both the substrate and particles, an additional deposition process was performed. Pre-heated powders were deposited onto the pre-heated IN718 substrate, which had been prepared by grinding the surface with P600 grade SiC sandpaper. Figure 7 presents the optical micrographs of the pre-heated IN718 substrate deposited with pre-heated IN718 powder particles. A uniform layer, approximately 160 μm in thickness, was successfully achieved, attributed to enhanced particle-to-particle interactions. It is noteworthy that the preheating treatment softened the powder particles and increased their deformability during the cold spray process, thereby facilitating the formation of a denser and thicker deposit.

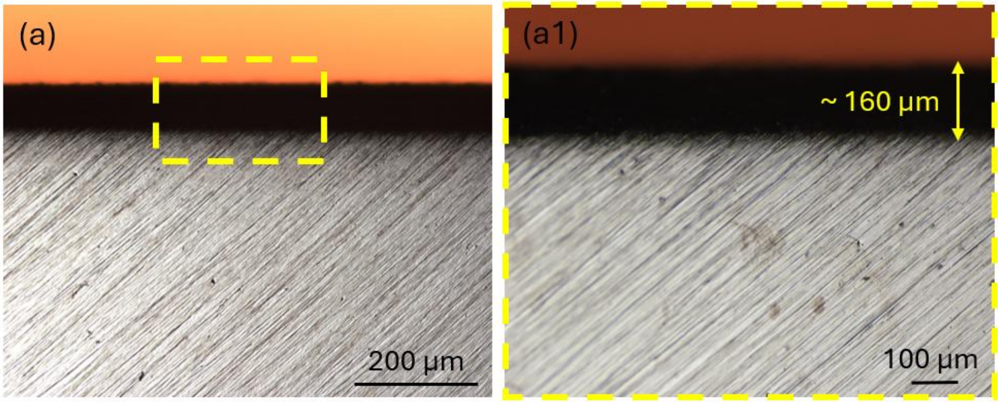

Figure 7. Optical images of the cold-spray deposited PH substrates, following powder preheating at 200 °C for 24 hours.

After achieving adhesion of the initial layer, the progression of the deposition is governed by the ability of the deposited particles to establish cohesive bonding. This bond is primarily determined by the mechanical response of the particles during their impact on the substrate. As shown in Figure 3, delamination of the deposited layers was observed in both ASF and PH samples, despite the enhanced interfacial bonding achieved for the PH substrates. It is important to note that the build-up of the deposition relies on successful particle-to-particle interactions or effective interparticle bonding. Analogous to the deposition of the initial layer, severe plastic deformation induces structural modifications in the particles, facilitating metallurgical bonding. With continued deformation, defects such as porosity and cracks are reduced, promoting particle compaction and enhancing the overall cohesion of the deposited layer [33]. Xie et al. [34] reported that pre-heated Fe powder demonstrated enhanced metallurgical bonding at inter-splat interfaces, accompanied by improved mechanical interlocking attributed to material jetting. These factors collectively contributed to a notable increase in ultimate tensile strength. Nevertheless, the ductility of the deposited substrate was adversely affected by the formation of nano-oxides on the pre-heated powder particles and the increased dislocation density. It is essential to emphasize that the formation of oxide particles or oxide films on the pre-heated powder surface impedes direct metal-to-metal contact between the particles and the substrate, thereby significantly diminishing the interfacial bonding strength and compromising the overall deposition quality [17].

Another critical aspect of powder preheating is the homogenization of the microstructure of as-received IN718 powder, which promotes enhanced metallurgical bonding during deposition. It is well established that gas-atomized powders generally exhibit dendritic structure resulting from the high cooling rates during processing, accompanied by the segregation of the solute atoms and the formation of brittle phases along interdendritic regions. Sabard and Hussain [35] carried out a solutionizing treatment on Al-6061 powder at 530 °C for 4 hours, followed by a thorough investigation of the resulting powder and deposition microstructures to elucidate the effects of the heat treatment process. Their findings revealed that reducing dislocation density and lattice defects, combined with the formation of large strain-free grains following solutionizing treatment, contributed to the formation of thicker deposits with reduced porosity.

3.3. Effect of Pre-heating and Deposition on the Phase Formation and Evolution

Figure 8(a) presents the XRD patterns of the powders and substrates both before and after the preheating treatment. The diffraction peaks were indexed to the face-centered cubic (FCC) γ-phase, corresponding to the (111), (200), (220), (311), and (222) crystallographic planes. Notably, no secondary phases such as γ″, γ′ or δ precipitates and carbides were detected following the heat treatment. Moreover, the (111) diffraction peak exhibited higher intensity in the powder samples, while the (200) peak was more pronounced in the substrates, irrespective of the pre-heating condition. On the other hand, XRD patterns of cold spray-deposited IN718 substrates prepared with different surface roughness conditions are given in Figure 8(b). Comparable phase compositions were observed across all samples, including both as-fabricated and pre-heated conditions.

Furthermore, the absence of oxidation-related peaks suggested that the cold spray process did not lead to significant phase transformations in the microstructure nor the formation of an oxide layer. As demonstrated, the dominance of the (111) diffraction plane in all coated samples indicated that the crystallographic texture of the deposited layer was closely aligned with that of the feedstock powder. Notably, cold spray processing induces intense plastic deformation at particle-substrate and particle-particle interfaces, often promoting the reorientation of grains toward low-energy configurations. In FCC metals, this deformation can cause grains to rotate, aligning the (111) planes with the substrate surface to minimize strain energy under high strain rates, as observed in Figure 8(b).

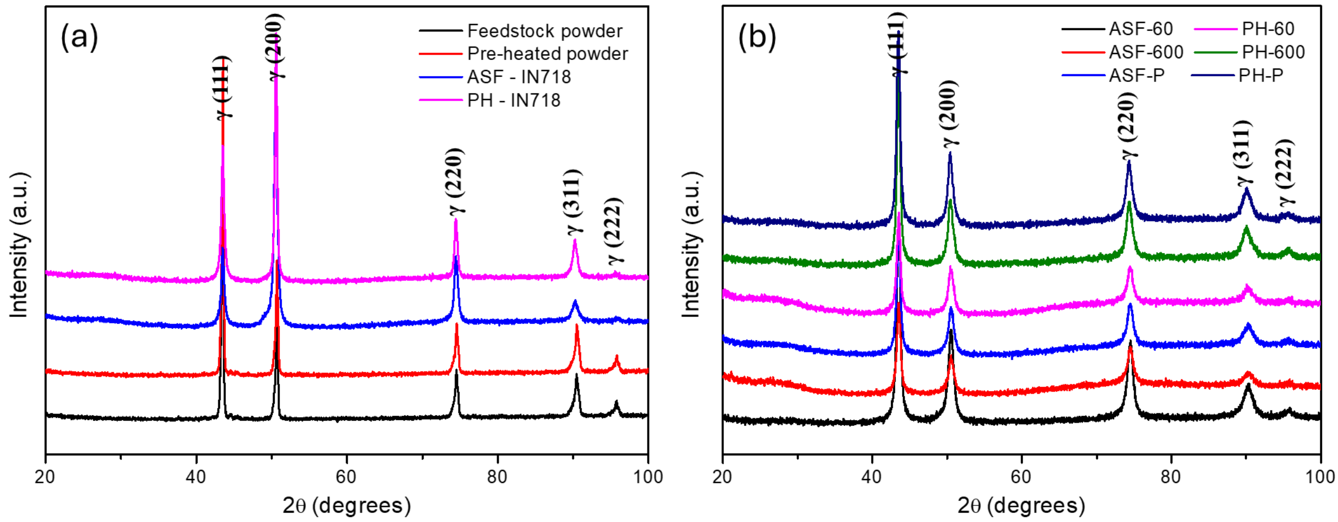

Figure 8. XRD patterns of IN718 powder and IN718 substrates: (a) before and after pre-heating treatment, and (b) following cold spray deposition processing.

4. Conclusions

The influence of surface condition and preheating on both the IN718 substrate and IN718 powder was evaluated concerning their deposition characteristics following cold spray processing. The primary findings of this study can be summarized as follows:

- The maximum deposition thickness was achieved for the ASF-600 and PH-600 substrates, indicating that a critical surface roughness is essential to facilitate effective interfacial bonding between the IN718 substrate and the non-preheated IN718 powder particles.
- All ASF substrates exhibited interfacial delamination and crack formation originating from the substrate surface, likely to be attributed to insufficient interfacial bonding. Conversely, these defects were localized to particular regions in the PH substrates, indicating improved bonding integrity.
- Preheating of the IN718 powder markedly enhanced the deposition quality, resulting in a substantial increase in thickness from 70 μm to 160 μm, despite identical surface conditions of the pre-heated IN718 substrates.
- XRD results confirmed the preservation of the FCC γ-phase without secondary phase formation or oxidation, while the dominance of the (111) peak in cold-sprayed samples indicated texture evolution driven by severe plastic deformation during deposition.

Acknowledgements

This research was supported by the Scientific and Technological Research Council of Turkey under the TUBITAK 2537- Czech Academy of Sciences, CAS Bilateral Cooperation Program with the Grant No: 123N951.

Declaration of Competing Interest

The authors declare that they have no known competing financial interests or personal relationships that could have appeared to influence the work reported in this paper.

Authorship Contribution Statement

Seren Özer: Writing – original draft, Writing – review & editing, Visualization, Methodology, Investigation, Data curation.
Merve Özkan: Writing – review & editing, Visualization, Methodology, Investigation, Data curation.
Arcan F. Dericioğlu: Writing – review & editing, Supervision, Methodology, Conceptualization.

References

[1] D. H. L. Seng et al., "Impact of spray angle and particle velocity in cold sprayed IN718 coatings," Surf. Coatings Technol., vol. 466, p. 129623, 2023, doi: 10.1016/j.surfcoat.2023.129623.
[2] P. Poza and M. A. Garrido-Maneiro, "Cold-sprayed coatings: Microstructure, mechanical properties, and wear behaviour," Prog. Mater. Sci., vol. 123, p. 100839, 2022.
[3] S. Bagherifard and M. Guagliano, "Fatigue performance of cold spray deposits: Coating, repair and additive manufacturing cases," Int. J. Fatigue, vol. 139, p. 105744, 2020, doi: 10.1016/j.ijfatigue.2020.105744.
[4] L. I. Pérez-Andrade, F. Gärtner, M. Villa-Vidaller, T. Klassen, J. Muñoz-Saldaña, and J. M. Alvarado-Orozco, "Optimization of Inconel 718 thick deposits by cold spray processing and annealing," Surf. Coatings Technol., vol. 378, p. 124997, 2019, doi: 10.1016/j.surfcoat.2019.124997.
[5] S. Bagherifard, S. Monti, M. V. Zuccoli, M. Riccio, J. Kondás, and M. Guagliano, "Cold spray deposition for additive manufacturing of freeform structural components compared to selective laser melting," Mater. Sci. Eng. A, vol. 721, pp. 339–350, 2018, doi: 10.1016/j.msea.2018.02.094.
[6] W. Ma et al., "Microstructural and mechanical properties of high-performance Inconel 718 alloy by cold spraying," J. Alloys Compd., vol. 792, pp. 456–467, 2019, doi: 10.1016/j.jallcom.2019.04.045.
[7] W. Li, K. Yang, S. Yin, X. Yang, Y. Xu, and R. Lupoi, "Solid-state additive manufacturing and repairing by cold spraying: A review," J. Mater. Sci. Technol., vol. 34, no. 3, pp. 440–457, 2018, doi: 10.1016/j.jmst.2017.09.015.
[8] S. Ozer, G. Mert, K. Davut, Z. Esen, and A. F. Dericioglu, "Effect of post fabrication aging treatment on the microstructure, crystallographic texture and elevated temperature mechanical properties of IN718 alloy fabricated by selective laser melting," J. Mater. Process. Tech., vol. 306, p. 117622, 2022, doi: 10.1016/j.jmatprotec.2022.117622.
[9] X. You et al., "Effect of solution heat treatment on the precipitation behavior and strengthening mechanisms of electron beam smelted Inconel 718 superalloy," Mater. Sci. Eng. A, vol. 689, no. 2, pp. 257–268, 2017, doi: 10.1016/j.msea.2017.01.093.
[10] K. Wang, Y. Liu, Z. Sun, J. Lin, Y. Lv, and B. Xu, "Microstructural evolution and mechanical properties of Inconel 718 superalloy thin wall fabricated by pulsed plasma arc additive manufacturing," J. Alloys Compd., vol. 819, p. 152936, 2020, doi: 10.1016/j.jallcom.2019.152936.
[11] S. Yin et al., "Cold spray additive manufacturing and repair: Fundamentals and applications," Addit. Manuf., vol. 21, no. August 2017, pp. 628–650, 2018, doi: 10.1016/j.addma.2018.04.017.
[12] G. Prashar and H. Vasudev, "A comprehensive review on the analysis of adhesion strength of cold spray deposits," Results in Surfaces and Interfaces, vol. 16, p. 100263, 2024, doi: 10.1016/j.rsurfi.2024.100263.
[13] A. Nourian and S. Müftü, "Effect of substrate surface finish and particle velocity on fatigue performance of cold spray coated A6061 aluminum alloy," Surf. Coatings Technol., vol. 444, p. 128676, 2022, doi: 10.1016/j.surfcoat.2022.128676.
[14] R. Singh et al., "Effects of substrate roughness and spray-angle on deposition behavior of cold-sprayed Inconel 718," Surf. Coatings Technol., vol. 319, pp. 249–259, 2017, doi: 10.1016/j.surfcoat.2017.03.072.
[15] M. Yu, W. Y. Li, F. F. Wang, X. K. Suo, and H. L. Liao, "Effect of particle and substrate preheating on particle deformation behavior in cold spraying," Surf. Coatings Technol., vol. 220, pp. 174–178, 2013, doi: 10.1016/j.surfcoat.2012.04.081.
[16] W. Sun et al., "Deposition characteristics of cold sprayed Inconel 718 particles on Inconel 718 substrates with different surface conditions," Mater. Sci. Eng. A, vol. 720, pp. 75–84, 2018, doi: 10.1016/j.msea.2018.02.059.
[17] Y. Xie et al., "Investigation on the influence of particle preheating temperature on bonding of cold-sprayed nickel coatings," Surf. Coatings Technol., vol. 318, pp. 99–105, 2017, doi: 10.1016/j.surfcoat.2016.09.037.
[18] D. Lee et al., "Correlation between microstructure and mechanical properties in additively manufactured Inconel 718 superalloys with low and high electron beam currents," J. Mater. Res. Technol., vol. 28, pp. 2410–2419, 2024, doi: 10.1016/j.jmrt.2023.12.184.
[19] D. Deng, J. Moverare, R. L. Peng, and H. Söderberg, "Microstructure and anisotropic mechanical properties of EBM

manufactured Inconel 718 and effects of post heat treatments," Mater. Sci. Eng. A, vol. 693, pp. 151–163, 2017, doi: 10.1016/j.msea.2017.03.085.

[20] S. Y. Im et al., "Unidirectional columnar microstructure and its effect on the enhanced creep resistance of selective electron beam melted Inconel 718," J. Alloys Compd., vol. 817, p. 153320, 2020, doi: 10.1016/j.jallcom.2019.153320.

[21] S. Kumar, G. Bae, and C. Lee, "Influence of substrate roughness on bonding mechanism in cold spray," Surf. Coatings Technol., vol. 304, pp. 592–605, 2016, doi: 10.1016/j.surfcoat.2016.07.082.

[22] T. S. Price, P. H. Shipway, and D. G. McCartney, "Effect of cold spray deposition of a titanium coating on fatigue behavior of a titanium alloy," Proc. Int. Therm. Spray Conf., vol. 15, pp. 507–512, 2006, doi: 10.1361/105996306X147108.

[23] A. Bisht, B. Alwin, M. Anantharaman, M. Kamaraj, and S. R. Bakshi, "Development of IN718 Coating for Repair Applications by High-Pressure Cold Spraying Followed by Heat Treatment," J. Therm. Spray Technol., vol. 33, no. 7, pp. 2242–2261, 2024, doi: 10.1007/s11666-024-01832-1.

[24] A. W. Y. Tan et al., "Effect of coating thickness on microstructure, mechanical properties and fracture behaviour of cold sprayed Ti6Al4V coatings on Ti6Al4V substrates," Surf. Coatings Technol., vol. 349, pp. 303–317, 2018, doi: 10.1016/j.surfcoat.2018.05.060.

[25] T. Marrocco, D. G. McCartney, P. H. Shipway, and A. J. Sturgeon, "Production of titanium deposits by cold-gas dynamic spray: Numerical modeling and experimental characterization," J. Therm. Spray Technol., vol. 15, no. 2, pp. 263–272, 2006, doi: 10.1361/105996306X108219.

[26] G. Prashar and H. Vasudev, "A comprehensive review on sustainable cold spray additive manufacturing: State of the art, challenges and future challenges," J. Clean. Prod., vol. 310, no. April, 2021, doi: 10.1016/j.jclepro.2021.127606.

[27] Y. Nikravesh, G. Frantziskonis, M. I. Latypov, and K. Muralidharan, "Atomistic characterization of impact bonding in cold spray deposition of copper," Materialia, vol. 28, p. 101736, 2023, doi: 10.1016/j.mtla.2023.101736.

[28] M. Winnicki, T. Piwowarczyk, and A. Małachowska, "General description of cold sprayed coatings formation and of their properties," Bull. Polish Acad. Sci. Tech. Sci., vol. 66, no. 3, pp. 301–310, 2018, doi: 10.24425/123436.

[29] A. Fardan, C. C. Berndt, and R. Ahmed, "Numerical modelling of particle impact and residual stresses in cold sprayed coatings: A review," Surf. Coatings Technol., vol. 409, p. 126835, 2021, doi: 10.1016/j.surfcoat.2021.126835.

[30] T. Hussain, D. G. McCartney, P. H. Shipway, and D. Zhang, "Bonding mechanisms in cold spraying: The contributions of metallurgical and mechanical components," J. Therm. Spray Technol., vol. 18, no. 3, pp. 364–379, 2009, doi: 10.1007/s11666-009-9298-1.

[31] A. Garfias et al., "Repair of Inconel 718 parts by Cold Spray Additive Manufacturing: The effect of substrate preheating on thick coatings properties," J. Alloys Compd., vol. 1010, p. 178182, 2025, doi: 10.1016/j.jallcom.2024.178182.

[32] S. Ozer, "Effect of post-processing heat treatment on the mechanical properties of Inconel 718 fabricated by selective laser melting," 2020.

[33] R. N. Raoelison, C. Verdy, and H. Liao, "Cold gas dynamic spray additive manufacturing today: Deposit possibilities, technological solutions and viable applications," Mater. Des., vol. 133, pp. 266–287, 2017, doi: 10.1016/j.matdes.2017.07.067.

[34] Y. Xie et al., "Improvement of tensile strength of cold sprayed Fe deposits via in-process powder preheating," Mater. Lett., vol. 316, p. 132090, 2022, doi: 10.1016/j.matlet.2022.132090.

[35] A. Sabard and T. Hussain, "Inter-particle bonding in cold spray deposition of a gas-atomised and a solution heat-treated Al 6061 powder," J. Mater. Sci., vol. 54, no. 18, pp. 12061–12078, 2019, doi: 10.1007/s10853-019-03736-w.